

Computation of internal voltage distribution in transformer windings by utilizing a voltage distribution factor

Andreas Theocharis, Marjan Popov and Vladimir Terzija

Abstract--In this paper, a method for the application of the black-box transformer models to the lumped-parameter transformer winding models is presented. The methodology is based on applying terminal transformer voltages as input parameters that could be provided by using the powerful black box vector fitting. Then, internal voltage distribution is determined by applying a lumped-parameter model approximation. In particular, the paper is focused on the direct computation of the internal voltage distribution, by avoiding a complicated procedure of solving the lumped-parameter winding model. The method is based on the transformation matrix utilization of the voltage distribution factors. This transformation matrix reflects the voltage distribution at specific internal points along the winding with respect to the input terminal voltages. At this stage, the inputs for the lumped-parameters model are provided by measured voltages at transformer terminals and the transformation matrix is determined through geometrical data of the transformer. The implementation of the proposed method with the black-box modeling approach in existing simulation software tools like EMTP is under development. The method is verified by comparing measured with computed waveforms.

Keywords: Lumped-parameters model, overvoltages, internal voltage distribution, transformer, transients, modelling.

I. INTRODUCTION

TRANSIENT overvoltages may occur as a consequence of the high-frequency interaction between the system and the transformer [1]-[6]. From the activities of Cigre Joint Working Group (A2/C4.39) has been concluded that when the natural frequency of a surge impulse matches the natural frequency of the system in which the transformer participates, a resonance in the system occurs [3], [4], [7]-[21]. Furthermore, when input surge impulses at transformer terminals cause internal transformer resonances, extreme overvoltages and finally insulation failures may occur [1], [14], [15].

This work was supported in part by the KPN project "Electromagnetic transients in future power systems (ref. 207160/E20)" financed by the Norwegian Research Council RENERGI program and a consortium of industry partners led by SINTEF Energy Research, Norway and Siemens AG. A. Theocharis is with Technological and Educational Institute of Western Greece, Faculty of Electrical Engineering, Patras 26334, Greece (e-mail: theochar@ece.upatras.gr).

M. Popov is with Delft University of Technology, Faculty EEMCS, Mekelweg 4, 2628CD, Delft, The Netherlands (e-mail: M.Popov@ieee.org).

V. Terzija is with University of Manchester, School of Electrical and Electronic Engineering, M13 9PL, Manchester, UK (e-mail: vladimir.terzija@manchester.ac.uk).

Paper submitted to the International Conference on Power Systems Transients (IPST2015) in Cavtat, Croatia June 15-18, 2015

Generally, three types of transformer models are distinguished for switching transient events. Transmission line models [22]-[28] are considered as an approach for very fast transients and voltage propagation studies [26]. They require very detailed design information of the transformer and they are time consuming. In addition, they cannot directly be implemented into electromagnetic transient software. The lumped-parameter models are used for the simulation of lightning impulses [29]-[35] and switching fast transients [14], [36]-[38]. These models can be used to study the interaction of the transformer with the surround network as well as to evaluate the internal voltage distribution [14], [39]. They can be implemented in electromagnetic transient software package [37]-[39] and are based on transformer geometrical data. The black box models are based on frequency admittance matrix measurement from any provided measuring point on the transformer winding [10]-[12], [16]-[21], [41]. These models are used to analyze the transformer interaction with the system and to study transferred overvoltages between terminals. In addition, they can be combined to existing simulation software tools like EMTP [16, 21] but however, they cannot determine the voltage propagation along the windings.

From the above, it is obvious that a reliable model for wide band terminal and internal switching transient overvoltage studies, which does not require accurate and detailed geometrical data, has not been established so far. At this point, the idea to combine black box transformer models, already implemented into EMTP-based software, to suitable lumped-parameter winding models for internal voltage distribution studies seems to be attractive [42], [43]. The terminal voltages computed from a black box model are used as inputs for the lumped-parameter model. That combination overcomes the disadvantage for a unified model suitable for terminal and internal transient overvoltage studies. Nevertheless, the drawback for detailed geometrical data remains. Moreover, the computation time could be significant because in the first step, the solution of the black-box model provides terminal currents and voltages and in the next step, the solution of the lumped-parameters model provides internal voltages. In order to overcome these disadvantages, on one hand, a method for direct internal voltage distribution computation needs to be established. On the other hand, that method has to be based on parameters that can be determined not only from geometrical data but also could be measured or calculated from several alternative methodologies.

In this paper, a method for direct computation, by avoiding digital solution of the lumped-parameter winding model, of

the internal voltage distribution is developed for given terminal transformer voltages. Furthermore, the method is based on the direct transformation of the terminal input voltages to internal voltage distribution by utilizing a transformation matrix that we will call a matrix of voltage distribution factors. The method is verified by laboratory measurements performed on a three-phase distribution transformer.

II. METHODOLOGY

The final equivalent electrical circuit of a transformer winding is derived with respect to winding geometry [15]. The final circuit is constructed as a connection of lumped-parameter blocks as shown in Fig. 1. Each block represents a segment of the winding. The segment could be one turn or a group of turns of the winding. The values of the lumped parameters of the blocks are computed by suitable methods as those given in [40]. For the equivalent circuit in Fig. 1, L_{si} , C_{si} and R_{si} , Y_{si} are the self-inductance, series capacitance and the associated series resistance and conductance as well as C_{shi} and Y_{shi} are the associated shunt capacitance and conductance to "reference" of the i^{th} block. For simplicity, the mutual inductive components are not shown in the figure. Usually, in order to avoid matrices of extremely large dimensions and long computation times, one segment corresponds to a number

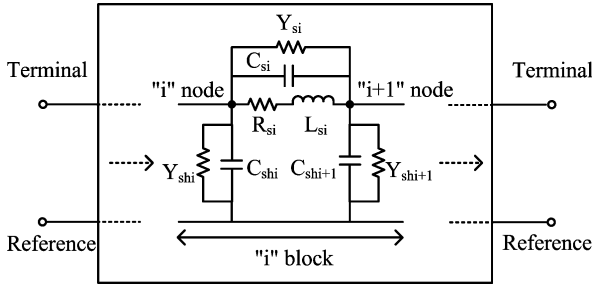


Fig. 1. The typical equivalent circuit block for internal voltage computations.

of winding's coils

By making use of the amplification factor [29], one can write that the amplification factor $N_{m,k}$ from an external node " t " to a particular internal node " m " with respect to the node " k " at which an input is applied is determined by

$$N_{m,k} = \frac{e_{t,k} - e_{m,k}}{e_{k,k}} \quad (1)$$

where e represents the node-to-reference voltage in frequency domain. In view of Fig. 1, $t=1$ or $t=n$, $m=1, \dots, n$ and k is an integer between 1 to n . The amplification factor $N_{m,k}$ depends on the winding structure and it can be computed in terms of the impedance matrix of the equivalent circuit in the Fig. 1. In this way and by the presumption that the input voltage is known and applied on winding terminals, the internal node voltage $e_{m,k}$ can be computed by

$$e_{m,k} = e_{t,k} - N_{m,k} e_{k,k} \quad (2).$$

The method is developed for a delta-wye transformer and is validated by measurements. At the delta side, terminal and

internal voltage measurements have been recorded during three-phase switching operation of the transformer through a vacuum circuit breaker (VCB). Because of the delta connection, a primary winding is excited by two impulses, each impulse at different phase terminal; for the input voltage at terminal "1" $t=1$, $m=1, \dots, n$ and $k=1$, and for the input voltage at terminal "n" $t=n$, $m=1, \dots, n$ and $k=n$.

Applying nodal analysis when the input is placed at terminal $t=1$

$$[e_{m,1}] = [Z_{ij}] [i_{m,1}] \quad (3)$$

where $[e_{m,1}] = [e_{1,1} \ e_{2,1} \ \dots \ e_{n,1}]^T$ the $n \times 1$ vector of the node voltages when the input is at terminal 1, $[Z_{ij}]$ with $i=1, \dots, n$ and $j=1, \dots, n$ is the $n \times n$ impedance matrix of the equivalent circuit in Fig. 1 and $[i_{m,1}] = [i_1 \ 0 \ \dots \ 0]^T$ $n \times 1$ is the vector of the source currents. By combining (1) and (3) one can easily derive the relation for the amplification factor in respect to the input at terminal "1" as

$$N_{1m,1} = 1 - \frac{Z_{m1}}{Z_{11}} \quad (4).$$

In the same way, the input is placed at terminal $t=n$

$$[e_{m,n}] = [Z_{ij}] [i_{m,n}] \quad (5)$$

where $[e_{m,n}] = [e_{1,n} \ e_{2,n} \ \dots \ e_{n,n}]^T$ is the $n \times 1$ vector of the node voltages when the input is at terminal n , $[Z_{ij}]$ with $i=1, \dots, n$ and $j=1, \dots, n$ is the $n \times n$ impedance matrix of the equivalent circuit in Fig. 1 and $[i_{m,n}] = [i_n \ 0 \ \dots \ 0]^T$ $n \times 1$ the vector of the source currents. The combination of (1) and (5) results in an amplification factor with respect to the input at terminal "n" as

$$N_{nm,n} = 1 - \frac{Z_{mn}}{Z_{nn}} \quad (6).$$

The node voltages of the delta connected winding can be expressed by superposition

$$[e_m] = [e_{m,1}] + [e_{m,n}] \quad (7)$$

By substituting (2) into (7) for the pair $t=1$ and $k=1$ as well as for the pair $t=n$ and $k=n$,

$$[e_m] = \begin{bmatrix} 1 - N_{11,1} \\ 1 - N_{12,1} \\ \vdots \\ 1 - N_{1n-1,1} \\ 1 - N_{1n,1} \end{bmatrix} e_{1,1} + \begin{bmatrix} 1 - N_{n1,n} \\ 1 - N_{n2,n} \\ \vdots \\ 1 - N_{nn-1,n} \\ 1 - N_{nn,n} \end{bmatrix} e_{n,n} \quad (8)$$

For the application of (8), the amplification terms are computed by (4) and (6). Moreover, $e_{1,1}$ and $e_{n,n}$ can be determined by the 2×2 system of equations consisting of the first and the last row in (8) for which e_1 and e_n are known in the frequency domain. The solution in matrix form is

$$\begin{bmatrix} e_{1,1} \\ e_{n,n} \end{bmatrix} = \begin{bmatrix} c_{11} & c_{1n} \\ c_{n1} & c_{nn} \end{bmatrix} \begin{bmatrix} e_1 \\ e_n \end{bmatrix} \quad (9)$$

By using (9) in (8), the internal node voltages are given by

$$\begin{bmatrix} e_m \end{bmatrix} = \begin{bmatrix} T_{m,1} & T_{m,14} \end{bmatrix} \begin{bmatrix} e_1 \\ e_n \end{bmatrix} \quad (10)$$

for $m=2, \dots, n-1$ and

$$\begin{bmatrix} T_{m,1} & T_{m,14} \end{bmatrix} = \begin{bmatrix} 1 - N_{12,1} \\ 1 - N_{13,1} \\ \vdots \\ 1 - N_{1n-2,1} \\ 1 - N_{1n-1,1} \end{bmatrix} \begin{bmatrix} c_{11} & c_{1n} \\ \vdots \\ c_{n1} & c_{nn} \end{bmatrix} \begin{bmatrix} 1 - N_{n2,n} \\ 1 - N_{n3,n} \\ \vdots \\ 1 - N_{nn-2,n} \\ 1 - N_{nn-1,n} \end{bmatrix} \quad (11)$$

The $(n-2) \times 2$ transformation matrix $\begin{bmatrix} T_{m,1} & T_{m,14} \end{bmatrix}$ expresses the voltage distribution at specific internal $n-2$ points along the winding in respect of the two input voltages e_1 and e_n and may be called as matrix of voltage distribution factors. The elements of the transformation matrix are frequency depended and can be computed through the elements of the $n \times n$ impedance matrix of the equivalent circuit that is used for the winding representation.

III. APPLICATION AND RESULTS

The proposed method of internal voltage distribution is applied in case of switching events for a GEAFOL cast-resin foil-winding transformer. The complete measurement setup consists of a feeder bus, a vacuum circuit breaker (VCB), a cable, a test transformer and a load. Switch-on and switch-off operations of the VCB have been performed and measured voltage waveforms have been recorded.

A. Description of the test transformer

The measurements have been conducted for a three-phase, 3.75MVA, 36.59/0.65 kV, delta-wye, core-type transformer. The windings at the primary side consist of 13 coils and each coil has approximately 90 foil-type turns. Apart of the terminal measuring points at both HV and LV sides, each primary winding is equipped by a special measuring point at the 90th turn. The most important geometrical parameters of the transformer are summarized in Table I. In view of Fig. 1, the 13 coils compose an equivalent circuit of $n=14$ nodes where nodes "1" and "14" are the terminal input nodes and the parameter $m=2, \dots, 12$.

TABLE I
TRANSFORMER DATA

	LV	HV
Turns sum	12	1170
Coils	1	13
Turns per coil	12	90
Inner diameter [mm]	376	655
Outer diameter [mm]	450	751
Strip [mm]	1.600x1200	0.400x71

B. Computation of the matrix of voltage distribution factors

The computation of the voltage distribution factors' matrix is accomplished through successful computation of the

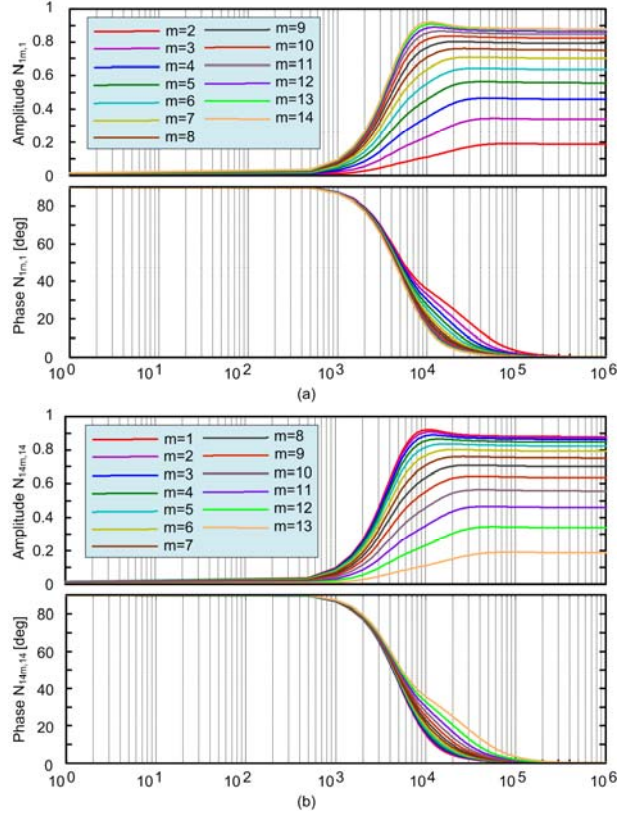


Fig. 2. The amplification factors in respect to: (a) terminal "1" and (b) terminal "14".

impedance matrix of the equivalent circuit in Fig. 1. According to [14], a valid approximation for the computation of the impedance matrix is

$$\begin{bmatrix} Z_{ij} \end{bmatrix} = \left(\begin{bmatrix} B_{ij} \end{bmatrix} + \begin{bmatrix} \Gamma_{ij} \end{bmatrix} \right)^{-1} \quad (12)$$

The matrices $\begin{bmatrix} B_{ij} \end{bmatrix}$ and $\begin{bmatrix} \Gamma_{ij} \end{bmatrix}$ are given by

$$\begin{bmatrix} B_{ij} \end{bmatrix} = (\omega \tan \delta + j\omega) \begin{bmatrix} C_{ij} \end{bmatrix} \quad (13)$$

$$\begin{bmatrix} \Gamma_{ij} \end{bmatrix} = \begin{bmatrix} k_{ij} \end{bmatrix} \left\{ \left(\sqrt{2\omega / \sigma \mu_0 d^2} + j\omega \right) \begin{bmatrix} L_{ij} \end{bmatrix} \right\}^{-1} \begin{bmatrix} k_{ij} \end{bmatrix}^T \quad (14)$$

where ω is the angular frequency, $\tan \delta$ is the loss tangent of the insulation dielectric losses factor, $\begin{bmatrix} C_{ij} \end{bmatrix}$ is the nodal capacitances matrix, $\begin{bmatrix} k_{ij} \end{bmatrix}$ is Kron's invariant transformation matrix [29]. $\begin{bmatrix} L_{ij} \end{bmatrix}$ is the inductances matrix in which core effects are included, d is the distance between the turns of the same coil, σ is the conductor conductivity and μ_0 is the magnetic permeability in vacuum. The computation of the nodal capacitance matrix and the inductance matrix is based on [15].

A dedicated code has been written in Matlab for the computations. The vector of angular frequencies is constructed that contains angular frequencies values up to 1 MHz with angular frequency step 100 Hz. For each one value of that vector, the impedance matrix $\begin{bmatrix} Z_{ij} \end{bmatrix}$ is computed using (12) for a high voltage (HV) winding of the transformer.

In the following step, the amplification factors $N_{1m,1}$ and

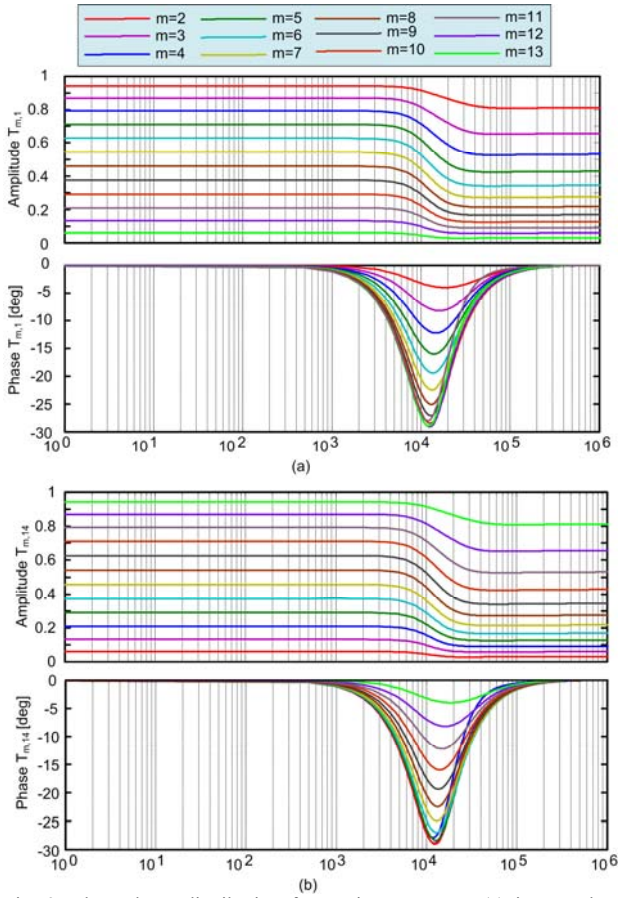


Fig. 3. The voltage distribution factors in respect to: (a) input voltage at terminal "1" and (b) input voltage at terminal "14".

$N_{14m,14}$ are computed using (4) and (6) and the results are shown in Fig. 2. The symmetrical construction of the winding leads to symmetrical impedance matrix and consequently symmetrical amplification factors with respect to the input terminals of the winding. Next, the elements of the 12x2 voltage distribution factors matrix are computed using (11) and the results are shown in Fig. 3. The same symmetry is observed for the voltage distribution factors as it was expected from the symmetry of the amplification factors.

C. Internal voltage distribution computation

Voltage measurements were recorded during three-phase closing and opening operations of a VCB connected to the loaded test transformer through a cable. Since the windings are connected in delta, the voltage of the last turn of a winding corresponds to the voltage of the first turn of the following winding. The winding inputs are the measured time domain waveforms at the winding terminals. Since the method computes the voltages in frequency domain, firstly the measured time domain input terminal waveforms must be transformed to frequency domain in order to define the vector of the angular frequencies for the computations. For verification, in order to be sure that the inverse Fourier transform is correctly performed, the measured and computed time domain waveforms at the winding terminals must have perfect matching. When the correct vector of the angular

frequencies has been determined, the matrix of voltage distribution factors is computed and finally the internal voltages are also computed by using (10).

In the case of closing operation of the VCB, the co-instantaneously measured waveforms and computed responses are presented in Fig. 4. In Fig. 4(a), the excellent matching between the measured and the computed waveforms at the winding terminals validates the correct performance of the Fourier transform. In Fig. 4(b), the internal voltage waveforms at the 90th turns for each one of the three windings are presented and the agreement with the measured values is very good. In particular, the computed rate of rise is in good agreement with the measured rate of rise. However, slight differences at the peak values for the winding between phases C and A are due to the electromagnetic compatibility issues because of the adjacency of many measuring wires. Moreover, differences between computed and measured values are due to that all measuring points cannot be reached directly onto the turn. A connection between the turn and the outside taps exists which is not reflected into the equivalent circuit in Fig. 1.

For opening operation of the VCB, the co-instantaneously measured waveforms and computed responses are presented in Fig. 5. In Fig. 5(a), the computed waveforms at the winding terminals validate the correct performance of the Fourier's transformations. In Fig. 5(b), the very good matching between the measured and the computed waveforms at the 90th turns for each one of the three windings validates the correct performance of the proposed method. Moreover, the computed rate of rise has good agreement with the measured rate of rise.

IV. CONCLUSIONS

The combination of black box transformer models to suitable lumped-parameters winding models provide grounds for the development of a unified model for terminal and internal voltage distribution studies. The terminal voltages computed from the black box model are inserted as inputs for the lumped-parameter model. However, the successful combination demands fast and direct voltage computations, especially after the computation of the input terminal voltages, as well as the avoidance of parameters determination from geometrical transformer data.

In this paper, a method for direct computation of the internal voltage distribution is presented by establishing the matrix of voltage distribution factors. This transformation matrix is invariant, its elements are frequency depended and reflects the internal properties and geometrical structure of the transformer winding. The application of the matrix of voltage distribution factors on the vector of the input terminal voltages derives the vector of internal voltages. The comparison of measured with the computed waveforms verifies that the high accuracy of the applied method for analyzing internal transient voltages during VCB transformer switching.

In the presented analysis, the method is developed for delta-wye connections of the transformer windings and the determination of the matrix of voltage distribution factors is based on geometrical data. This work opens new horizons in terms of:

- the methodology can be applied for any kind of winding connections,
- several options should be established for the determination

- of the transformation matrix using geometrical data, measurements or both options and
- more work should be done in order to make this approach

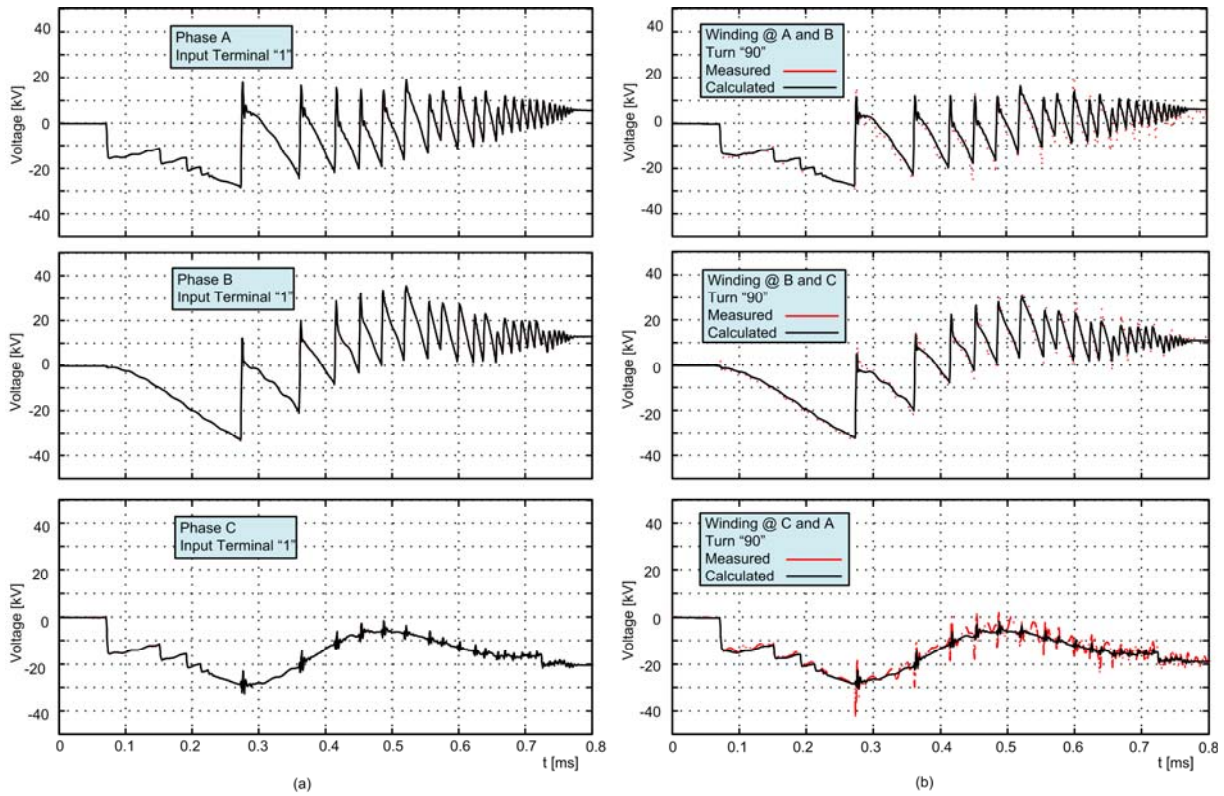


Fig. 4. Measured and computed voltages for closing operation of the VCB at the three windings at the phases A, B and C at: (a) terminals of the windings and (b) 90th turns in the windings.

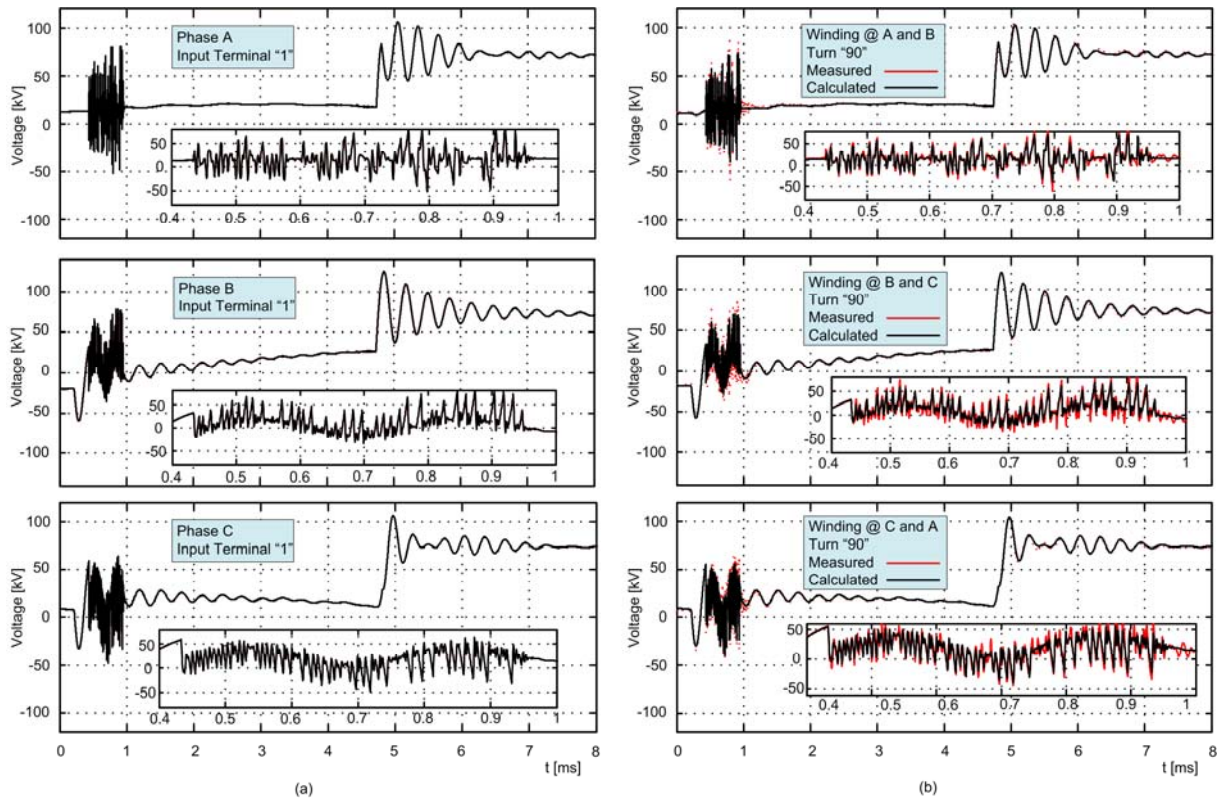


Fig. 5. Measured and computed voltages for opening operation of the VCB at the three windings at the phases A, B and C at: (a) terminals of the windings and (b) 90th turns in the windings.

possible for implementation in an electromagnetic transient program environment.

The complete unification of the black-box and lumped-parameter modeling is still under investigation and improvements are going to be presented in future work.

V. REFERENCES

- [1] R. Malewski, J. Douville, and L. Lavalee, "Measurement of switching transients in 735-kV substations and assessment of their severity for transformer insulation," *IEEE Trans. Power Del.*, vol. 3, no. 4, October 1988, pp. 1380-1387.
- [2] J. Declercq, "Transformers for wind turbines need for new designing or business as usual," presented at the 17th Int. Conf. Elect. Distrib., Barcelona, Spain, May 2003.
- [3] R. Asano, A.C.O. Rocha, G. M. Bastos, "Electrical transient interaction between transformers and the power system," Cigré-33, Cigré Brazil JWG A2/C4-03, Brugge 2007.
- [4] A.C.O. Rocha, "Electrical transient interaction between transformers and the power system", Cigré C4-104, Cigré Brazil JWG A2/C4-03, Paris 2008.
- [5] D. D. Shipp, T. J. Dionise, V. Lorch, and B. J. MacFarlane, "Transformer failure due to circuit breaker induced transients," *IEEE Trans. Ind. App.*, vol. 47, no. 2, pp. 707-718, March/April 2011.
- [6] T. Abdulahovic, "Analysis of high-frequency electrical transients in offshore wind parks," PhD Dissertation, Department of Energy and Environment, Chalmers Univ. Technol., Goteborg, Sweden, 2011.
- [7] *Electrical Transient Interaction Between Transformer and the Power System, Part-1: Expertise*, Joint Working Group A2/C4.39, Cigre, April 2014.
- [8] *Electrical Transient Interaction Between Transformer and the Power System, Part-1: Expertise*, Joint Working Group A2/C4.39, Cigre, April 2014.
- [9] P. Mukherjee, L. Satish, "Construction of equivalent circuit of a transformer winding from driving-point impedance function analytical approach", *IET Electr. Power Appl.*, vol. 6, no. 3, pp. 172-180, 2012.
- [10] B. Gustavsen, "Study of transformer resonant overvoltages caused by cable-transformer high-frequency interaction," *IEEE Trans. Power Del.*, vol. 25, no. 2, pp. 770-779, April 2010.
- [11] B. Gustavsen, A. P. Brede, and J. O. Tande, "Multivariate analysis of transformer resonant overvoltages in powers station," *IEEE Trans. Power Del.*, vol. 26, no. 4, October 2011, pp. 2563-2572.
- [12] B. Badrzadeh and B. Gustavsen, "High-frequency modeling and simulation of wind turbine transformer with doubly fed asynchronous generators," *IEEE Trans. Power Del.*, vol. 27, pp. 770-779, April 2012.
- [13] G. Stein: "A Study of the Initial Surge Distribution in Concentric Transformer Windings", *AIEE Transaction*, September 1964, pp. 877-892.
- [14] M. Popov, R. P. P. Smeets, L. van der Sluis, H. de Herdt, and J. Declercq, "Experimental and theoretical analysis of vacuum circuit breaker prestrike effect on a transformer," *IEEE Trans. Power Del.*, vol. 24, no. 3, July 2009, pp. 1266-1274.
- [15] M. Popov, B. Gustavsen, and J. A. Martinez-Velasco, "Transformer modeling for impulse voltage distribution and terminal transient analysis," in *Electromagnetic Transients in Transformer and Rotating Machines Windings*, 1st ed. Hershey, Pennsylvania, USA.
- [16] A. O. Soysal, and A. Semlyen, "Practical transfer function estimation and its application to wide frequency range presentation of transformers," *IEEE Trans. Power Del.*, vol. 8, no. 3, July 1993, pp. 1627-1637.
- [17] B. Gustavsen, and A. Semlyen, "Application of the vector-fitting to the state equation representation of transformers simulation of electromagnetic transients," *IEEE Trans. Power Del.*, vol. 13, no. 3, July 1998, pp. 834-842.
- [18] B. Gustavsen, and A. Semlyen, "Rational Approximation of Frequency Domain Responses by Vector Fitting," *IEEE Trans. Power Del.*, vol. 14, no. 3, July 1999, pp. 1052-1061.
- [19] B. Gustavsen, "Computer Code for Rational Approximation of Frequency Dependent Admittance Matrices," *IEEE Trans. Power Del.*, vol. 17, no. 4, October 2002, pp. 1093-1098.
- [20] B. Gustavsen, "Wide band modelling of power transformers," *IEEE Trans. Power Del.*, vol. 26, no. 4, October 2011, pp. 2563-2572.
- [21] A. Morched, L. Marti, and J. Ottevangers, "A high frequency transformer model for EMTP," *IEEE Trans. Power Del.*, vol. 8, no. 3, July 1993, pp. 1615-1626.
- [22] Y. Shibuya, S. Fujita, N. Hosokawa, "Analysis of Very Fast Transient Overvoltages in Transformer Winding", *IEEE Proc Gen. Trans. Distr.*, vol. 144, no. 5, September 1997, pp. 461-468.
- [23] Y. Shibuya, S. Fujita, E. Tamaki, "Analysis of very fast transient in transformers", *IEEE Proc Gen. Trans. Distr.*, vol. 148, no. 5, September 2001, pp. 377-383.
- [24] M. Popov, L. van der Sluis, R. P. P. Smeets, J. L. Roldan, "Analysis of very fast transients in layer-type transformer windings," *IEEE Trans. Power Del.*, vol. 22, no. 1, January 2007, pp. 238-247.
- [25] M. Popov, L. van der Sluis, G.C. Paap, H. de Herdt, "Computation of very fast Transient overvoltages in transformer windings", *IEEE Trans. Power Del.*, vol. 18, no. 4, October 2003, pp. 1268-1274.
- [26] M. Popov, L. van der Sluis, R.P.P. Smeets, J.L. Roldan, and V. Terzija, "Modelling simulation and measurement of very transients in transformer windings with consideration of frequency-dependent losses," *IET Electr. Power Appl.*, vol. 1, no. 1, January 2007, pp. 29-35.
- [27] M. Popov, L. van der Sluis, and R. P. P. Smeets, "Evaluation of surge-transferred overvoltages in distribution transformers," *IET Electr. Power Syst. Res.*, vol. 78, 2008, pp. 441-449.
- [28] Makarand M. Kane, and S. V. Kulkarni, "MTL-based analysis to distinguish high-frequency behavior of interleaved windings in power transformers," *IEEE Trans. Power Del.*, vol. 28, no. 4, October 2013, pp. 2291-2299.
- [29] R. C. Degeneff, "A general method for determining resonances in transformer windings", *IEEE Trans. Power App. Syst.*, PAS-76, no. 2, March/April 1977, pp. 423-430.
- [30] J. H. McWhirter, C. D. Fahrnkopf, and J. H. Steele, "Determination of impulse stresses within transformer windings by computer", *AIEE Trans.*, 75, (III), 1957, pp. 1267-1274.
- [31] P. I. Fergestad, and T. Henriksen, "Transient oscillations in multiwinding transformers", *IEEE Trans. Power App. Syst.*, vol. 93, no. 2, 1974, pp. 500-509.
- [32] A. Miki, T. Hosoya, and K. Okuyama, "A calculation method for pulse voltage distribution and transferred voltage in transformer windings," *IEEE Trans. Power App. Syst.*, vol. PAS-97, no. 3, 1978, pp. 930-939.
- [33] W. J. McNutt, T. J. Blalock, and R. A. Hinton, "Response of transformer windings to system transient voltages," *IEEE Trans. Power App. Syst.*, vol. PAS-93, pp. 457-467, 1974.
- [34] T. Teranishi, M. Ikeda, M. Honda, T. Yanari, "Local voltage oscillation in interleaved transformer windings," *IEEE Trans. Power App. Syst.*, vol. 100, no. 2, 1981, pp. 973-881.
- [35] Y. Shibuya, and S. Fujita, "High-frequency model of transformer winding," *Elect. Eng. Japan*, vol. 146, no. 3, 2004, pp. 8-15.
- [36] R. C. Degeneff, W. J. McNutt, W. Neugebauer, J. Panck, J., M. E. McCallum, and C. C. Honey, "Transformer response to system switching voltages," *IEEE Trans. Power App. Syst.*, 101, (6), 1982, pp. 1457-1470
- [37] R.C. Dugan, R. Gabrick, J.C. Wright, and K.V. Pattern, "Validated techniques for modeling shell-form EHV Transformers", *IEEE Trans. Power Del.*, vol. 4, no. 2, April 1989, pp. 1070-1078.
- [38] Y. Yang, Z. J. Wang, X. Cai, and Z. D. Wang, "Improved lumped parameter model for transformer fast transient simulations," *IET Electr. Power Appl.*, vol. 5, no. 6, 2011, pp. 479-485.
- [39] D.J. Wilcox: "Theory of Transformer Modelling Using Modal Analysis," *Proc. Inst. Elect. Eng. C*, vol. 138, no. 2, March 1991, pp. 121-128.
- [40] V. Rashtchil, E. Rahimpour, H. Shahrouzi, "Model reduction of transformer detailed R-C-L-M model using the imperialist competitive algorithm", *IET Electr. Power Appl.*, vol. 6, no. 4, pp. 233-242, 2012.
- [41] D. Filipovic-Grcic, B. Filipovic-Grcic, and I. Uglesic, "High-Frequency Model of the Power Transformer Based on Frequency-Response Measurements," *IEEE Trans. Power Del.*, vol. 30, no. 1, pp. 34-42, Feb. 2015.
- [42] G. H. Oliveira and S. D. Mitchel, "Comparison of black-box modelling approaches for transient analysis: A GIS substation case study," in *Proc. 2013 International Conference on Power Systems Transient 2013, IPST 2013*.
- [43] S. D. Mitchel and J. S. Welsh, "Initial parameters estimates and constrains to support gray-box modelling of power transformers," *IEEE Trans. Power Del.*, vol. 28, no. 4, October 2013, pp. 2411 - 2418.